

Determination of Different Types of Fractures Utilizing Shallow and Deep Resistivity and Characterization of Abu Roach C Reservoir, Bed-15 Field, Abu El Gharadig Basin, North Western Desert, Egypt

Fatma Yehia<sup>1,2</sup>, A. Z. Noah<sup>1</sup>, M. M. Abu Heleika<sup>2</sup>, Khalid I. Kabel<sup>1</sup>, T. Shazly<sup>1</sup>

<sup>1</sup> Egyptian Petroleum Research Institute (EPRI), Nasr City, Cairo, Egypt

<sup>2</sup> Minia University, Faculty of Science, Geology Department, Minia, Egypt

Received June 22, 2021; Accepted January 14, 2022

## Abstract

One of the most significant basins in the Egyptian North Western Desert is Abu El Gharadig basin. This basin contains a huge subsurface sedimentary zone. This paper aims to determine vertical and horizontal fractures and their parameters by utilizing shallow and deep resistivity logs. This technique is dependent upon the separation between shallow and deep resistivity regarding vertical fractures, and sharp reduction of LLS log regarding horizontal fractures. If the mud's conductivity is identified, the estimation of fracture aperture can be achieved in a high-contrast composition. Furthermore, to guarantee the fracture type, the dipping of the observed fracture is estimated. Reservoir characterization parameters for seven wells are established for the reservoir performance of "Abu Roach" "C Member" in the specified area. The gained results managed to determine vertical and horizontal fractures where the apertures range of vertical fractures is (2-47mm), whilst the apertures range of horizontal fractures is (31-48mm). Fracture dipping (Y) range is (0.831-3.3mm) for vertical and is (-5.8 to -0.9mm) for horizontal. Porosity ranges from 0.003 to 0.052 for wells. The petrophysical parameters show that Abu Roach (C) is the main reservoir in studied area with optimum porosity and permeability, and needs more developed to achieve more production.

**Keywords:** Reservoir characterization; Porosity; Permeability; Vertical fractures; Horizontal fractures; Shallow and deep resistivity.

## 1. Introduction

This study aimed to determine vertical and horizontal fractures and their parameters (aperture, dipping, and porosity) utilizing shallow and deep resistivity logs, and with the accessible well logs data, the reservoir petrophysical parameters for seven wells (Bed 15-1, Bed 15-2, Bed 15-3, Bed 15-7, Bed 15-7A, Bed 15-8, Bed 15-9) were calculated to demonstrate the reservoir performance of "Abu Roach" "C Member" in the specified area. These examined wells are located in the BED-15 Field that is a section of Badr-El-Din concession which is located in the Western Desert, about 300 KM west of Cairo and about 100 KM west of Bed-1 working field. The north-western sector of Abu El Gharadig basin between latitudes 29° 45' and 30° 05' N, and between longitudes 27° 30' and 28° 10' E serves as the study area. The map showing the location of the chosen study wells is observed in Fig.(1), and these wells are marked with red. Fractures are mostly discovered in hardened and fragile formations which are commonly located sub-vertical and perpendicular to the plane of a group of seemingly parallel fractures [1].

While vertical fractures suggest high-angle events (aligned with the borehole), horizontal fractures involve actual horizontal or sub-horizontal events [2]. Detection of fracture in friable rocks near boreholes is considered by many [3-6]. Regarding log interpretation, the two (shallow and deep) logs demonstrated a degree of deviation in front of fractures from the usual conditions, where mud simply replaces the initial fluid if open fractures are found. These deflections were utilized to determine the types of fractures along with their apertures, dipping

and porosities. The shallow resistivity (RLLS) is separated from the deep resistivity (RLLD) by the action of vertical fractures, where RLLD is superior to RLLS ( $RLLD > RLLS$ ). Alternatively, horizontal fracture caused abrupt reduction in the deep laterolog (RLLD) regardless of separation which can even be reversed ( $RLLS > RLLD$ ).

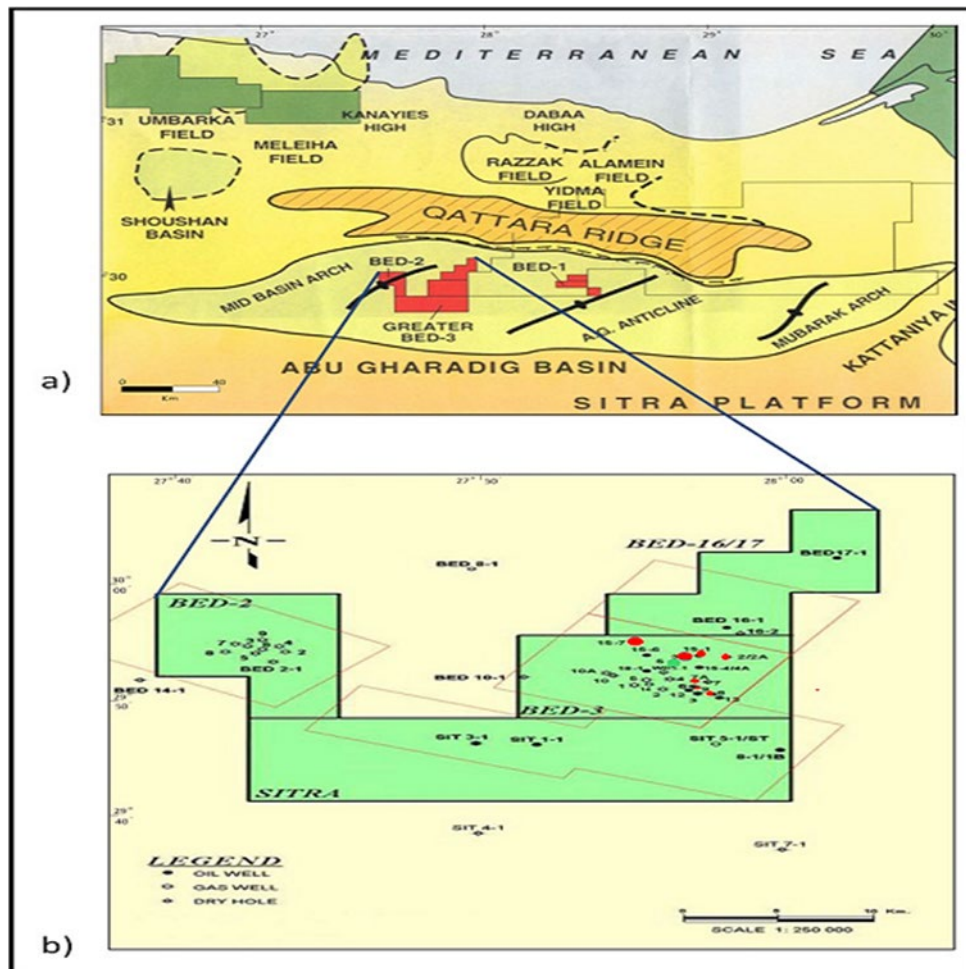


Fig.1. Location map showing the studied wells [10]

Compared with vertical fractures, the separation in the case of horizontal fractures was insignificant [7]. Furthermore, regarding the available well logs for reservoir characterization, Gamma Ray is used to determine shale volume (Vsh) which is crucial for characterization of the reservoir because shale existence in any composition can be a serious obstacle in determining the formation porosity and the included fluid saturation [8-9].

Finally, the characteristics of the reservoir regarding lithology identification, petrophysical parameters, fluid distribution and porosity type depend on shale volume estimation. These parameters are crucial to determine effective and total porosity, water saturation, and hence the reservoir potentiality. By utilizing software programs, other petrophysical logs parameters such as neutron and density were calculated.

## 2. Subsurface stratigraphy

The Egyptian northwest Desert has a thick stratigraphic succession, and it contains the majority of the sedimentary sequence from Pre-Cambrian substructure complex to the recent one [10-11] as demonstrated in Fig. (2).

The stratigraphic sequence [12] contains cycles of alternate depositions of carbonates and Clastics. There are five cycles which have been known as the follows:

- A clastic facies cycle which predominates the most ancient sedimentary rocks, and it contains Lower Jurassic and Palaeozoic formations.
- A section of carbonate which is of Upper and Middle Jurassic formations.
- A clastics cycle which contains Lower Cretaceous all the way to Upper Cretaceous Early Cenomanian.
- Repeatedly, carbonate depositions are distributed all over the northwest Desert from Upper Cenomanian all the way up to the Middle Eocene.
- The most superficial cycle of clastic depositions contains Upper Eocene Oligocene, Miocene and a more immature section.

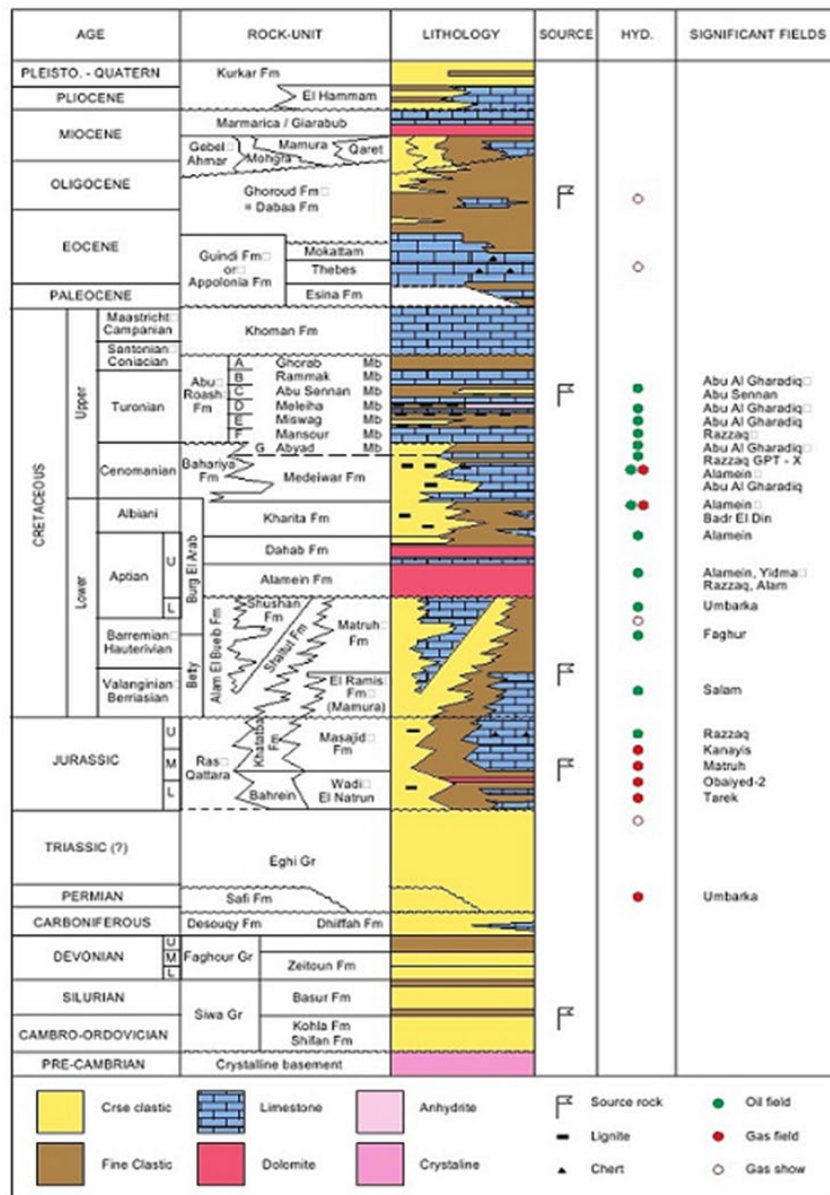


Fig.2. Generalized Litho-Stratigraphic Column of the North Western Desert [16-17]

The principal study area is Abu Roach "C" Member (Turonian) which is primarily consists of shale, sandstone, and siltstone containing some streaks of limestone; this was precipitated in a shallow confined marine shelf [13]. In Abu El Gharadig basin, Abu Roach "C" was precipitated

in the Late Cretaceous (Turonian) as a piece of a whole transgression which began in Cenomanian (Bahariya Formation) and came to an end in Maastrichtian (Khoman Formation) [13]. The sand of Abu Roach reservoir was composed through increased supply of clastic from the basin southern border which was initially covered by massive lagoons [14].

### 3. Determination of fracture types and its parameters

The measures of resistivity with variant examination depths have been determined by two logs which are shallow (LLS) and deep (LLD) resistivity. These investigation depths are dependent on the rock resistivity and on the contrast resistivity between the fractured and the un-fractured zones.

The measurements of resistivity can be extremely affected by the sort and saturation of water-dependent mud. Moreover, adjustments are inquired for borehole size and bed thickness. Based upon these effects, sequence of mathematical simulations has formed charts to produce the exact log estimations [15]. It is mostly required to incorporate resistivity tools to be used in lower porosities, salt muds and high-resistivity formations [16-17].

#### 3.1. Fracture types

The vertical fracture calculation is determined by the division between shallow and deep resistivity logs, where  $R_{LLD} < R_{LLS}$  (Fig. 3a), whilst the separated horizontal fracture can be estimated by the abrupt reduction in LLD (Fig. 3b). These variations in the log calculations were utilized to discover the locations of vertical and horizontal fractures.

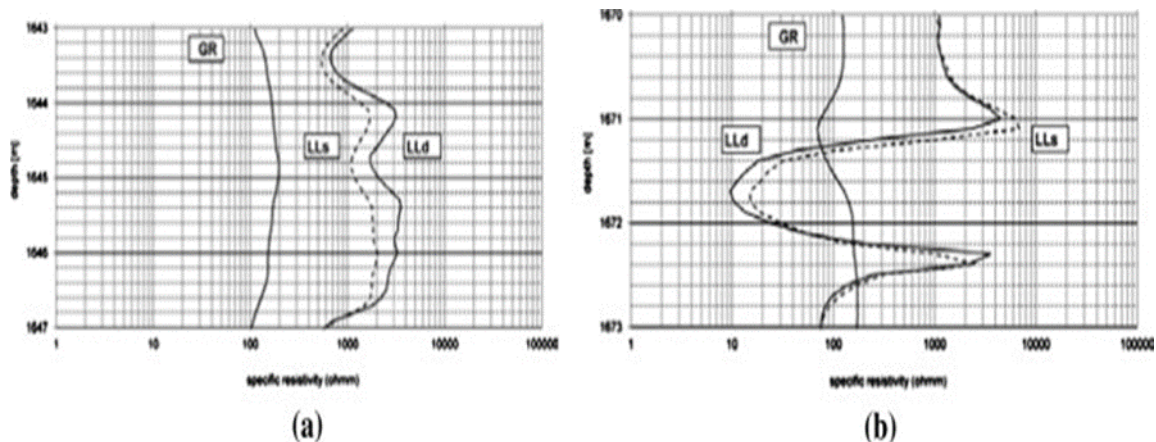


Fig. 3. The Resistivity logs response near a vertical fracture and a single horizontal fracture

The dislocation of mud to replace the original fluids, which is observed in the open fractures, is the cause of these differences in log readings. The various fractures in the studied formations were located by utilizing resistivity logs for the seven wells of study.

#### 3.2. Fracture apertures

Between deep and shallow resistivity curves, massive separations are detected in fractured rocks. The reaction of the log in high-contrast formations is managed by four parameters which are: the formation blocks resistivity ( $R_b$ ), the invading fluid resistivity ( $R_m$ ), and the degree of invasion and fracture opening. Utilizing some simplified expectations, a finite-element numerical model has been established to measure the dual laterolog in the borehole, which is used to resolve the problem of inversion and to find the fracture aperture.

Regarding vertical apertures, the difference in conductivity ( $\Delta c$ ) between shallow and deep laterolog (CLLS and CLLD) was needed to calculate the fracture aperture [19-19]. In vertical fractures, the exact amount ( $\Delta c$ ) appeared to be equivalent to the whole fracture opening, in which the implemented equations were dependent upon the used formula [20]. On the other hand, regarding horizontal fractures, the deep resistivity was observed to be reduced quickly,



which may or may not produce reversed separation between LLD and LLS. The difference in conductivity between the deep laterolog (CLLD) and the matrix of the un-fractured block ( $C_b$ ) is directly proportional to the sum of horizontal fracture aperture and the conductivity of the invading fluid ( $C_m$ ). These are shown in the following equations [20]:

- Vertical apertures

$$\Delta c = 4 \cdot 10^{-4} \varepsilon_v \cdot C_m \quad (1)$$

$$\varepsilon_v = (C_{LLS} - C_{LLD}) / (4 \cdot 10^{-4} \cdot C_m) \quad (2)$$

- Horizontal apertures

$$C_{LLD} - C_b = 1.2 \cdot 10^{-4} \varepsilon_h \cdot C_m \quad (3)$$

$$\varepsilon_h = (C_{LLD} - C_b) / (1.2 \cdot 10^{-4} \cdot C_m) \quad (4)$$

where:  $C_{LLS}$  and  $C_{LLD}$  are measured directly by dual laterolog;  $\Delta c$  is the conductivity difference in Ohm m;  $\varepsilon_v$  is the vertical fracture aperture in micrometer ( $\mu m$ );  $C_m$  is the mud conductivity measured in the borehole in Ohm  $m^{-1}$ ;  $\varepsilon_h$  is the horizontal fracture aperture ( $\mu m$ ),  $C_b$  is the conductivity of the non-fractured host rock; it is calculated from  $R_b$  which may be different from  $R_t$ .

The maximum values of  $R_{LLD}$  can be used as  $R_b$  in zones of non-fractured rock masses [20].

### 3.3. Fracture porosity

An equation can calculate the fracture porosity [21]. The correlation between the formation total porosity and both of formation resistivity and formation water resistivity determines the power function. Archie's equation has been found to calculate the fracture porosity in hard formations, and it is as the follows [20]:

$$\Phi_{frac}^m = (C_{LLD} - C_{LLS}) / C_m \quad (5)$$

where:  $\Phi_{frac}$  is the fracture porosity;  $m$  is the Archie's cementation exponent, (mostly about 2),. Also cementation factor is less than two in case of fractured formations;  $C_{LLS} = 1/R_{LLS}$  is the conductivity measured by the shallow laterolog;  $C_{LLD} = 1/R_{LLD}$  is the conductivity measured by the deep laterolog;  $C_m = 1/R_m$  is the mud conductivity measured by mud log(7).

### 3.4. Fracture dipping

The parameter "Y" can be calculated by [22] the equation (6) which finds the fracture dip. If "Y" is greater than 0.1, sub-vertical fracture is found; when "Y" is between 0 and 0.1, a dipping fracture is located; and provided that "Y" is lower than 0, sub-horizontal fracture is detected.

$$Y = \frac{R_{LLD} - R_{LLS}}{\sqrt{R_{LLD} \times R_{LLS}}} \quad (6)$$

## 4. Reservoir characterization using available well logging

Reservoir parameters (shale volume, total and effective porosities and water saturation) are determined by utilizing the available well logs (Gamma Ray, porosity logs (Neutron and density), shallow and deep resistivity). Software is used to estimate the shale volume of the reservoir of study. As per Schlumberger techniques to determine the minimum value of shale volume, it was observed that Gamma Ray log calculation is the minimum value used to estimate the shale volume [23].

### 4.1. Volume of shale

One of the most preferred tools used to determine and calculate the shale volume is Gamma Ray log [24]. This is mainly because it sensitively responds to radioactive materials which are commonly found in high concentrations in shaly formations; an equation is used to find the Gamma Ray index [25]. Moreover, the shale volume is adjusted [26-27] formulated to achieve the best values of shale used in the log analysis.

Afterwards, the various zones were categorized to clean, shaly, and shale zones, according to the following:

- If  $V_{sh} < 10\%$ , this indicates a clean zone;
- If  $V_{sh}$  is between 10% and 35%, this indicated a shaly zone;
- If  $V_{sh} > 35\%$ , this indicates a shale zone.

## 4.2. Determination of total and effective porosities

They are commonly expressed in percentages. Values of porosity can be identified by porosity tools which contain density, sonic and neutron.

The compensated log of the formation density can calculate the rock density ( $P_b$ ), and the compensated sonic log of the borehole calculates the internal transit time through the rock ( $\Delta t$ ), and the neutron porosity log was utilized to calculate the formation hydrogen index and to find the neutron porosity.

While there are three known porosity logs types (density, sonic and neutron), the total and effective porosities were estimated using only density and neutron in this study.

### 4.2.1. Density log:

It is one of the most reliable tools to estimate the formation porosity because of the insignificant effect of argillaceous matter, if present, in its response. Porosity obtained from density log can be estimated in clean and shaly zones. In clean zones, the porosities derived from density log ( $\phi_D$ ) are determined by the relation shown in the equation [28]. In shaly zones, the formula of (25) is utilized to calculate the total porosity.

### 4.2.2. Neutron log

In clean zones, the porosity values ( $\phi_{CNL}$ ) are directly given by neutron logs. However, in shaly zones, neutron porosity can be adjusted due to the influence of the implied shale. The adjusted porosity, determined by the neutron log, can be calculated by Allen's equation [29], and the adjusted neutron and density porosities can be estimated from the equations [30].

## 4.3. Determination of fluid saturation

Water saturation ( $S_w$ ) is the portion of bore area holding water. Hydrocarbon saturation ( $S_h$ ) is the term given to the remaining portion containing gas or oil, and it equals  $(1-S_w)$ .

Regarding the estimation of the water saturation below the predominant subsurface geologic conditions in the area of study, a number of the utilized techniques will be outlined in this section [8].

In this paper, water saturation ( $S_w$ ) was calculated utilizing the Indonesian [31] model. Equations [32] are used in this model to compute un-invaded zone and flushed-zone water saturation.

## 5. Results and discussion

### 5.1. Application of fracture identification in the area of study

The earlier technique that utilized deep and shallow resistivity logs to determine vertical and horizontal fractures was implemented in Abu Roach "C" Member for detecting the parameters of these fractures in the chosen formation of the area of concern in the northwest Desert. The various fracture parameters are demonstrated in (Table 1). Additionally, the logs raw data for discovering vertical and horizontal fractures found in the wells of study is illustrated as the follows:

- In Bed 15-1 well of Abu Roach "C" Member, the vertical fractures were documented, and they showed a multitude of vertical fractures that expanded from the depths between 3145 m to 3150 m. The greatest aperture approached 17  $\mu\text{m}$ . The fracture porosity value is equal to 0.003, and the "Y" parameter is 0.831 for vertical fractures without any horizontal ones. Furthermore, in Bed 15-2 well of Abu Roach "C" Member, two horizontal fractures were discovered with an aperture of average 500  $\mu\text{m}$ , and "Y" value is equivalent to -5.81 without evidence of vertical fractures.
- In Bed 15-3 well of Abu Roach "C" Member, horizontal and vertical fractures were computed. One horizontal fracture has been found at a depth of 3134 m with an aperture approaching 361  $\mu\text{m}$ , and a massive number of vertical fractures was found with apertures ranging from 2  $\mu\text{m}$  to 5  $\mu\text{m}$ . The fracture porosity is around 0.002, and regarding the dipping factor, it is -0.9 for the horizontal fracture and 1.61 for the vertical ones. However,

Bed 15-7 well of Abu Roach "C" Member does not contain any vertical or horizontal fractures.

- In Bed 15-7A well of Abu Roach "C" Member, two fractures were detected. There is one horizontal fracture located at 3638 m depth with an aperture of 500  $\mu\text{m}$ , and the other one is vertical with an aperture of 10  $\mu\text{m}$ . regarding the dipping factor values, they are -0.2 for the horizontal fracture and 0.6 for the vertical one. The fracture porosity of this well is around 0.003. In addition to this, Bed 15-8 well of Abu Roach "C" Member contains one horizontal and three vertical fractures. The horizontal fracture is located at 3179 m depth with an aperture of about 416  $\mu\text{m}$ , while the three vertical fractures have apertures ranging from 11  $\mu\text{m}$  to 40  $\mu\text{m}$ . The fracture porosity is around 0.01, and the dipping factors are -0.1 and 3.1 for the horizontal and vertical fractures respectively.
- Lastly, in Bed 15-9 well of Abu Roach "C" Member, there are two horizontal and two vertical fractures. The two horizontal fractures have an aperture that measures about 450  $\mu\text{m}$  with a "Y" value of -0.5. The two vertical fractures are located at depths of 3125 m and 3188 m with apertures that range from 3  $\mu\text{m}$  to 47  $\mu\text{m}$ , and their dipping value is 2.1. The fracture porosity of this well of study is 0.052.

Table 1. The Estimated fracture parameters for the different wells in the studied area

Well Name	Fracture Porosity	Horizontal Fracture		Vertical Fracture	
		Aperture	Y Factor	Aperture	Y Factor
Bed15-1	0.003	-	-	2-17mm	0.831
Bed15-2	0.022	31-481mm	-5.8	-	-
Bed15-3	0.002	361mm	-0.9	2-5 mm	1.6
Bed15-7	-	-	-	-	-
Bed15-7A	0.003	500 mm	-0.2	10 mm	0.6
Bed15-8	0.01	416 mm	-0.1	11-40 mm	3.1
Bed15-9	0.052	63-451 mm	-0.5	3-47 mm	2.1

## 5.2. Characterization of Abu Roach C reservoir

To identify the quality of the reservoir, it is crucial to consider the petrophysical parameters such as the shale volume, effective and total porosity, and water saturation of the formation containing the gas or oil. Utilizing the below surfer 2013 that shows the petrophysical parameters distribution through the area of study, the available logs of these parameters were identified and explained.

### 5.2.1. Shale volume and effective porosity distribution maps

The distribution map of shale volume in Abu Roach "C" Member is demonstrated in (Fig. 4) which shows variable values of shale content with the minimum value of (10.6%) in Bed 15-3 well and the maximum value of (26.8%) in Bed 15-7 well. Principally, the content of shale distribution diminishes towards the centre with the minimum value found at the centre of the area of study.

Regarding the distribution map of the effective porosity in Abu Roach "C" Member, it is shown in (Fig. 5) displaying the minimum value of (17.6%) in Bed 15-7 well and the maximum value of (30%) in Bed 15-3 well. Generally, the effective porosity increases all around towards the centre of the area of study.

### 5.2.2. Water saturation distribution map

The distribution map of water saturation in Abu Roach "C" Member (Fig.6) demonstrates different values of water saturation with the minimum value of (16.7%) in Bed 15-3 well and the maximum value of (46.4%) in Bed 15-1 well. Water saturation distribution generally increases towards the northeast and south parts of the area of study.

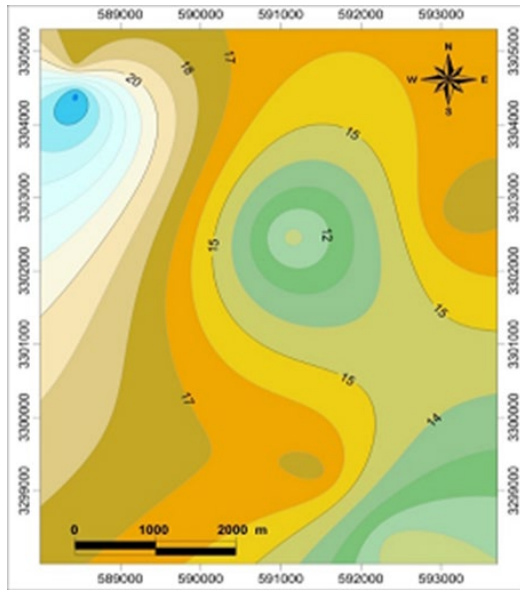


Fig.4. Shale volume distribution map of the studied area

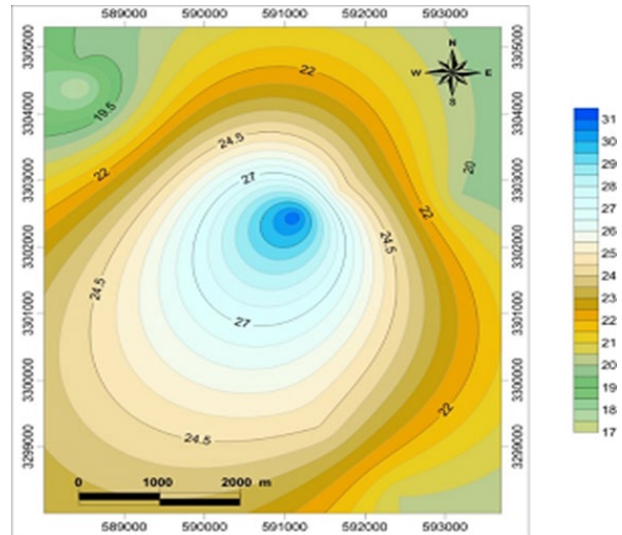


Fig.5. Effective porosity distribution map of the studied area

### 5.2.3. Hydrocarbon saturation distribution map

The distribution map of hydrocarbon saturation in Abu Roach "C" Member (Fig.7) exhibits variations in the values of hydrocarbon saturation with the minimum value of (53.6%) in Bed 15-1 well and the maximum value of (83.3%) in Bed 15-3 well. Generally, the hydrocarbon saturation rises from all directions towards the centre of the area of study.

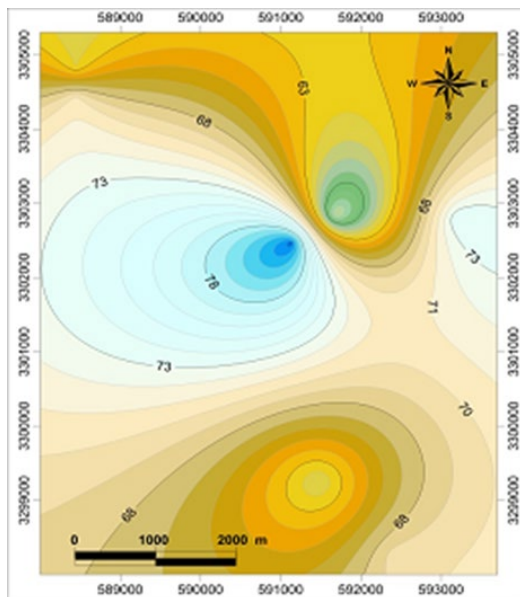


Fig.6. Water saturation distribution map of the studied area

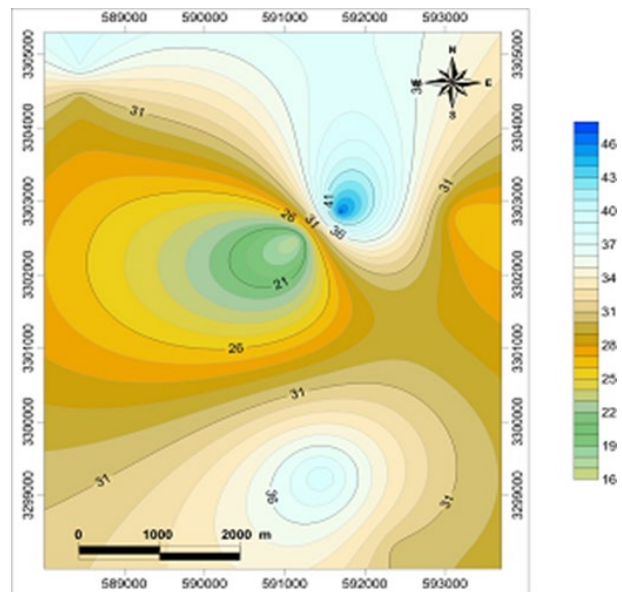


Fig.7. Hydrocarbon saturation distribution map of the studied area



#### 5.2.4. Net Pay thickness distribution map

In a definite scale, the distribution map of the net pay thickness in Abu Roach "C" Member shows similar distribution for net reservoir thickness. The distribution pattern indicates that the western and central areas of Abu Roach "C" Member are more promising locations for more hydrocarbon exploration. Finally, a summary of petrophysical parameters for Abu Roach "C" Member reservoir is shown in (Table 2).

Table 2. Summary of petrophysical parameters for Abu Roash C reservoir zone

Well name	Top	Bottom	AV.PHI	AV.VSH	AV.SW	AV.SH
BED 15-1	3077	3162	25	12.6	46.4	53.6
BED15-2	3144	3231	20	17.6	26	74
BED15-3	3063	3146	30	10.6	16.7	83.3
BED15-7	3165.5	3249.5	17.4	26.8	29.6	70.4
BED15-7A	3505.5	3642	19.6	17.6	38	62
BED 15-8	3164	3208	20.5	11	30.5	69.5
BED 15-9	3125	3209.5	24.4	17.3	39	61

## 6. Summary and conclusion

In Abu Roach "C" Member Reservoir, the petrophysical parameters (shale volume, water saturation, effective porosity, hydrocarbon saturation, and net pay thickness) were computed by using surfer 2013 and software 2015 programs. The quantitative assessments show that net thickness of the reservoir is principally located in the western, the eastern and the central areas, while the net pay distribution in the pattern points to the western and the central areas. This is because they possess average values of effective porosity (22%), shale volume (16.2%), and water saturation (42%).

As a result of the previous discussion, it is recognized that Bed 15-3 is characterized as a promising reservoir because it has a high permeability, low shale content, and large number of vertical and horizontal fractures. However, Bed 15-7 and Bed 15-2 wells possess low permeability, high shale content, and two vertical and horizontal fractures only in Bed 15-2 well. Finally, Bed 15-7 well does not contain any vertical or horizontal fractures. Furthermore, we recommend that more development and improvement are needed for Bed 15-3 well to guarantee more production.

### Acknowledgment

*Thanks for Academy of Scientific Research and Technology (ASRT) for funding the research thesis "Effect of nanomaterials to induce fractures within sandstone and carbonate reservoirs for Abu Roash C and F members Badr El-Din area north western desert Egypt".*

*Thanks for EPRI (Egyptian Petroleum Research Institute) for giving me the chance to get M.Sc. and their great support.*

### References

- [1] Noah AZ, Shazly TF. Integration of well logging analysis with petrophysical laboratory measurements for Nukhul Formation at Lagia-8 well, Sinai, Egypt. *Am J Res Commun.*, 2014; 2(2):139–66.
- [2] Shazly TF, Tarabees E. Using of Dual Laterolog to detect fracture parameters for Nubia Sandstone Formation in Rudeis-Sidri area, Gulf of Suez, Egypt. *Egyptian Journal of Petroleum*, 2013;22(2):313–9.
- [3] Minne JC, Gartner J. Fracture detection in the Middle East. In: *Middle East Technical Conference and Exhibition*, Society of Petroleum Engineers; 1979.
- [4] Aguilera R. *Naturally fractured reservoirs*. 1980;
- [5] van Golf-Racht TD. *Fundamentals of fractured reservoir engineering*. Elsevier; 1982.

- [6] Shazly TF, Abd Elaziz W. Petrophysical evaluation of the Upper Cretaceous section in Abu Rudeis-Sidri Area, Gulf of Suez, Egypt using well logging data. *J Appl Geophys.*, 2010; 7:1–14.
- [7] Vasvari V. On the applicability of Dual Laterolog for the determination of fracture parameters in hard rock aquifers. *Austrian Journal of Earth Sciences*, 2011; 104(2):80–9.
- [8] Shazly TF, Nouh AZ. Determination of some reservoir characteristics of the Bahariya Formation in Bed-1 Field, Western Desert, Egypt, by using the repeat formation tester. *Petroleum science and technology*, 2013; 31(7): 763–74.
- [9] El-Ata A. C. Lithology make-up identification and determination, using well, logging analysis: Clays Model. *Bull, of GSOGE*. 1989;23: 241–67.
- [10] Moustafa AR. Mesozoic-Cenozoic basin evolution in the northern Western Desert of Egypt. 2008;
- [11] Shazly TF, Ramadan MAM. Well logs application in determining the impact of mineral types and proportions on the reservoir performance of Bahariya formation of Bassel-1x well, western desert, Egypt. *Journal of American Science*, 2011;7(1): 498–505.
- [12] EGPC. Exploration And Production Review (Part 1), Western Desert, Oil And Gas Fields,. In: (A Comprehensive Overview) EGPC, Cairo,. 1992. p. 431p.
- [13] Said R. The geology of Egypt. Routledge; 2017.
- [14] Mansour A, Gentzis T, El Nady MM, Mostafa F, Tahoun SS. Hydrocarbon potential of the Albian-early Cenomanian formations (Kharita-Bahariya) in the North Western Desert, Egypt: A review. *Journal of Petroleum Science and Engineering*, 2020; 107440.
- [15] East SM. Geology of Egypt. In: *Well Evaluation Conference*, Egypt. 1984. p. 1–64.
- [16] Atlas W. Introduction to wireline log analysis. Western Atlas International Inc, Houston, Texas. 1995;
- [17] Fricke S, Schön J. *Praktische Bohrlochgeophysik*. Enke im Georg Thieme Verlag; 1999.
- [18] Boyeldieu C, Winchester A. Use of the Dual Laterolog for the evaluation of the fracture porosity in hard carbonate formations. 1982;
- [19] Shaaban Y. "Reservoir Evaluation Of Nubia S.S. Formation, In Rudeis-Sidri Area, Gulf Of Suez, Egypt, Utilizing Well Log Interpretation.", *Sohag Univ.*; 2010.
- [20] Sibbit AM, Faivre O. The dual laterolog response in fractured rocks. In: *SPWLA 26th Annual Logging Symposium*. Society of Petrophysicists and Well-Log Analysts; 1985.
- [21] Archie GE. "The electrical resistivity logs as an Aid in determining some reservoir characteristics." *Trans. AIM*, 1942;; 54-67.
- [22] Deng S, Wang X, Zou D, Fan Y, Yang Z. Interpreting dual laterolog fracture data in fractured carbonate formation. *Journal of China University of Geosciences*, 2006; 17(2): 168–72.
- [23] Mahmoud M, Ghorab M, Shazly T, Shibl A, Abuhagaza AA. Reservoir characterization utilizing the well logging analysis of Abu Madi Formation, Nile Delta, Egypt. *Egyptian Journal of Petroleum*, 2017; 26(3): 649–59.
- [24] El-Khadragy AA, Shazly TF, Ramadan M, El-Sawy MZ. Petrophysical investigations to both Rudeis and Kareem formations, Ras Ghara oil field, Gulf of Suez, Egypt. *Egyptian Journal of Petroleum*, 2017; 26(2): 269–77.
- [25] Dresser A. Log interpretation charts. Houston, Dresser Industries Inc. 1979;
- [26] Clavier C, Coates G, Dumanoir J. Theoretical and experimental bases for the dual-water model for interpretation of shaly sands. *Society of Petroleum Engineers Journal*. 1984; 24(02): 153–68.
- [27] Steiber RG. Optimization of shale volumes in open hole logs. *Journal of Petroleum Technology*, 1973; 31(1973): 147–62.
- [28] Wyllie MRJ, Gregory AR, Gardner GHF. An experimental investigation of factors affecting elastic wave velocities in porous media. *Geophysics*, 1958; 23(3): 459–93.
- [29] Allen LS, Mills WR, Caldwell RL. The effects of fluid invasion in pulsed neutron logging. *Geophysics*, 1965; 30(3): 389–95.
- [30] Limited S. *The Essentials of Log Interpretation Practice*. Services Techniques Schlumberger; 1972.
- [31] Leveaux J, Poupon A. Evaluation of water saturation in shaly formations. *The Log Analyst*, 1971; 12(04).
- [32] Schlumberger. *Techlog program software manual operating*.

To whom correspondence should be addressed: Fatma Yehia Mohamed Khawas, Egyptian Petroleum Research Institute (EPRI), Nasr City, Cairo, Egypt, E-mail: [fatmayehia93@outlook.com](mailto:fatmayehia93@outlook.com)  
ORCID ID: 0000-0003-0201-3457